DIFFUSION OF CORONENE AND PORPHINES IN POROUS CATALYST SUPPORTS

Gon Seo* and Hee Moon

Department of Chemical Engineering, Chonnam National University, Kwangju, Chonnam 500, Korea

(Received 21 May 1985 • accepted 25 July 1985)

Abstract—Effective diffusivities and counter-diffusivities of coronene and porphines dissolved in organic solvents were measured in alumina and silica alumina catalyst supports. The measured effective diffusivity was in the range of $10^{-11}-10^{-10}$ m^2/s and the counter-diffusivity, $10^{-15}-10^{-14}$ m^2/s.

Very small values of counter-diffusivities indicated that the flux of adsorbate desorbed was greatly decreased by the flow of desorbate formed in the opposite direction. Experimental results showed that diffusivities of porphines in aluminas increased with strength of adsorption. One of the possible explanation for this result was that the strongly adsorbed molecules have the shielding effect on diffusing molecules through pore fluid.

INTRODUCTION

The intraparticle diffusion in catalyst supports has been the subject of a number of investigations on catalytic reactions. Since porous catalysts are manufactured by impregnation on a support by solutions containing the active metal ions, the structure of the support influences the final catalytic porperty. Studies on the diffusion within catalyst supports [1-5], therefore, have given valuable information in analyzing the reaction rate on porous supported catalysts. Particularly, in the liquid-phase reaction such as the hydrodesulfurization to remove sulfur-containing polyaromatic compounds in heavy oils, the intraparticle diffusion should be considered since it is usually the rate-controlling step.

When the transport of molecules is controlled by the pore diffusion through the pore fluid, the mass transfer rate is affected sensitively by the ratio of the molecular diameter to the pore diameter, $\lambda\,(=d_m/d_p)$. Chantong [1] reported that effective diffusivities of aromatic compounds in aluminas decreased exponentially with the increase in λ, indicating the strong steric hindrance and the hydrodynamic drag. Seo and Massoth [2] studied the effect of temperature and pressure on the effective diffusivity in the same system. They showed that the temperature dependency on the effective diffusivity was significant, while the effect of pressure was negligible up to 70 atm.

In catalytic reactions, there are always two flows in pores; reactants diffuse into catalyst particles and products formed diffuse out. From the physical point of view, therefore, the use of effective diffusivity for analyzing the kinetic data is not likely to be adequate in systems where reactions occur within porous particles. This situation has been called as "counter-diffusion" [3].

This paper describes a method to determine the counter-diffusivity in porous catalyst supports. Counter-diffusion runs were carried out by measuring the amount of coronene and porphines desorbed after a desorbate such as acetone or pyridine was injected into the reaction vessel. Counter-diffusivities of coronene and porphines in alumina supports were determined by applying the analytical solution of counter-diffusion model to the experimental uptake data. In this study, the effects of the temperature, the diameter ratio (λ), the adsorbate or desorbate concentration and the strength of adsorption between molecules and supports will be also studied to ascertain the mechanism of diffusion and the interaction between diffusing molecules and pore walls.

THEORETICAL DIFFUSION MODELS

Pore Diffusion Model

For combined diffusion and adsorption in the spherical particle, the mass balance equation for a solute may be represented by the following equation [4]:

$$\varepsilon \frac{\partial C_r}{\partial t} = D_e\left(\frac{\partial^2 C_r}{\partial r^2} + \frac{2}{r}\frac{\partial C_r}{\partial r}\right) - \rho\frac{\partial q}{\partial t} \tag{1}$$

Initial and boundary conditions are:

$$\text{(I. C.)}\quad C_r = C_0 \quad \text{at } t=0 \quad \text{for } 0<r<R \tag{2}$$

$$\text{(B. C.)}\quad \frac{\partial C_r}{\partial r} = 0 \quad \text{at } r=0,\ t>0 \tag{3}$$

* To whom all correspondence should be directed.

$$V\left(\frac{\partial C_r}{\partial t}\right) = -4\pi R^2 N_p D_e \left(\frac{\partial C_r}{\partial r}\right) \quad \text{at} \quad r=R, \quad t>0 \tag{4}$$

If the adsorption isotherm is linear, the apparent diffusivity can be defined as follows:

$$D_a = D_e/(\rho K+\varepsilon) \tag{5}$$

where K is the adsorption equilibrium constant.
Then, Eq. (1) can be rewritten by:

$$\frac{\partial C_r}{\partial t} = D_a\left(\frac{\partial^2 C_r}{\partial r^2}+\frac{2}{r}\frac{\partial C_r}{\partial r}\right) \tag{6}$$

The solution of Eq. (6) was presented in the literature [6].

$$\frac{q}{q_\infty} = 1-\sum_{n=1}^{\infty}\frac{6\alpha(\alpha+1)\exp(-q_n^2\tau)}{\alpha^2 q_n^2+9\alpha+9} \tag{7}$$

where α is $C_\infty/(C_1-C_\infty)$ and τ is a dimensionless time defined as:

$$\tau = D_a t/R^2 \tag{8}$$

q_n in Eq. (7) are roots of the following transcendental function:

$$\tan q_n = 3q_n/(3+\alpha q_n) \tag{9}$$

Here, we did not deal with non-linear adsorption isotherms. In the case of non-linear isotherms, numerical solutions are available [1].

The effective diffusivity, D_e, was determined by an usual method. At first, q/q_∞ should be evaluated from Eq. (7) for a certain value of τ. Then, the time, t, was determined from experimental uptake curves so that q/q_∞ has the same value. After obtaining some sets of τ and t, a plot of τ against t could be prepared. This plot should yield a straight line if the intraparticle transport follows the pore diffusion model. Figure 1 shows such a plot for a diffusion run with tetra-phenylporphine. The apparent diffusivity could be obtained from the slope of the plot using a least-square method. Finally, the effective diffusivity was evaluated from the apparent diffusivity by using Eq. (5).

Counter-Diffusion Model

In counter-diffusion runs, the preadsorbed aromatic compound was desorbed by injecting a certain amount of desorbate into the vessel. Acetone and pyridine were used as desorbates since they have very small molecular size and strong adsorptivity to aluminas. Thus, the desorbate diffuses fast into pores and the desorption of aromatic compounds on the pore surface takes place instantly. The following assumptions were made in the mathematical modelling of the counter-diffusion [7].

i) Since the desorbate has a strong adsorptivity and diffuses very fast into pores, the desorption of aromatics occurs instantly within the particle.

ii) The initial concentration of aromatic compounds desorbed inside the particle may be calculated as follows:

$$C_0 = (q_{eq}-q_{re})/\left(\frac{4}{3}N_p\pi R^3\varepsilon\right) \tag{10}$$

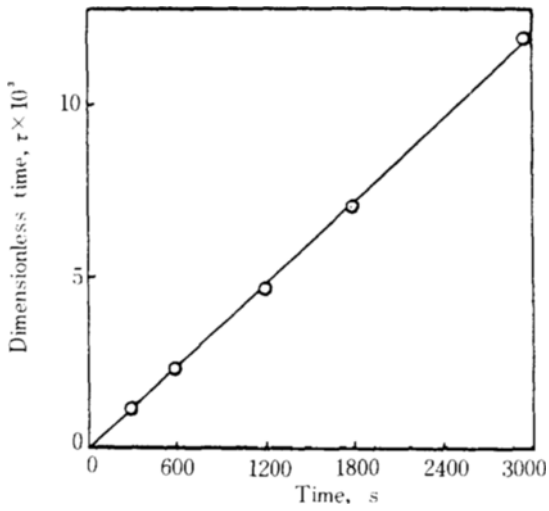

Fig. 1. Typical plot of τ against t.

Under these assumptions, the material balance equation on the aromatic compound within the particle may be written as follows:

$$\varepsilon\frac{\partial C_r}{\partial t} = D_{ec}\left(\frac{\partial^2 C_r}{\partial r^2}+\frac{2}{r}\frac{\partial C_r}{\partial r}\right) \tag{11}$$

Initial and boundary conditions are:

$$\text{(I. C.)} \quad C_r = C_0 \quad \text{at} \quad t=0 \quad \text{for} \quad 0<r<R \tag{12}$$

$$\text{(B. C.)} \quad \frac{\partial C_r}{\partial r} = 0 \quad \text{at} \quad r=0, \quad t>0 \tag{13}$$

$$V\frac{\partial C_t}{\partial t} = -4\pi R^2 N_p D_{ec}\left(\frac{\partial C_r}{\partial r}\right) \quad \text{at} \quad r=R, \quad t>0 \tag{14}$$

$$C_t = C_1 \quad \text{at} \quad t=0 \tag{15}$$

Equation (11) can be solved analytically by the similar method used by Crank [6]. The solution is expressed as:

$$\frac{C_t-C_1}{C_\infty-C_1} = 1-\sum_{n=1}^{\infty}\frac{6\alpha(\alpha+1)\exp(-q_n^2\tau)}{\alpha^2 q_n^2+9\alpha+9} \tag{16}$$

In this case, α is defined as $C_\infty/(C_0-C_\infty)$ and τ is $D_{ec}\,t/R^2\,\varepsilon$. The counter-diffusivity, D_{ec}, was obtained by the same procedures described previously.

EXPERIMENTAL

Adsorbates and Adsorbents

Adsorbates used here are reagent grade coronene

Table 1. Physical properties of adsorbents.

	Aluminas				Silica-aluminas	
	UC 1	UC 2	D**	M**	SA-13	SA-23
Surface area* $\times 10^{-3}$, m^2/kg	280	220	245	320	400	420
Average pore diameter*, nm	5	9	9.8	7.2	9	6
Particle density, kg/m^3	1080	900	1210	1220	700	920
Porosity	0.76	0.90	0.73	0.71	0.81	0.70

* Data were provided from manufacturers
** from Chantong and Massoth[4]

and tetra-phenylporphine (TPP) manufactured by the Tokyo Kasei Co. and octa-ethylporphine (OEP) by Man-Win Co. The critical molecular diameters of coronene, TPP and OEP are 1.11, 1.9 and 1.53 nm, respectively. Solutions were prepared by resolving a certain amount of adsorbates in n-hexane and cyclohexane which are not adsorbed strongly on alumina [1]. The solvents were pretreated with calcined molecular sieves 5A to remove water and other impurities.

Adsorbents are porous catalyst supports, aluminas and silica-aluminas. Aluminas, UC1 and UC2, were provided by the United Catalyst Inc. and aluminas, D and M, by the Kaiser Aluminium Co.. Silica-aluminas, SA-13 and SA-23 were provided by the Davidson Chemical Co. The physical properties of adsorbents are shown in Table I. The pore volume and the density were measured by the helium-mercury penetration method. Adsorbent particles used were passed through a 35 mesh sieve and retained on a 65 mesh sieve (Tyler screen). The arithmetic average of the two sieve openings was taken as the particle diameter. The average particle diameter was 0.315×10^{-3}m.

Diffusion Experiments

The diffusion runs were conducted in the stirred batch vessel similar to that used by Seo [7]. The vessel was made of stainless steel and four fixed baffles spaced evenly around the circumference. The agitation was achieved with a teflon rod connected to a variable speed motor. The solution temperature inside the vessel was controlled by inserting the vessel into a constant temperature water jacket. The water in the jacket was circulated by a Haake circulator held at a given temperature. The solution temperature was maintained at a certain value within ± 0.5K. A known weight of the alumina was calcined at 823 K for 18 hours in the muffle furnace. The calcined alumina was then transfered into solvents in order to prevent moisture uptake. The solution of a certain concentration was put into the vessel and, at a designated starting time, the alumina in solvent was transfered into the solution in the vessel and the stirrer was operated. Liquid samples were taken periodically to monitor the change in concentration of the solution by using a hyperdermic syringe. The concentrations of the samples were measured with a UV-VIS spectrophotometer at wavelengthes of 328 nm for coronene, 512 nm for TPP and 500 nm for OEP. In the counter-diffusion runs, a desorbate was injected into the vessel after the equilibrium of porphine between the solution and the adsorbent has been reached. The injected amount of acetone as a desorbate was about $0.5\times10^{-6}m^3$, an excess amount for desorbing preadsorbed aromatic compounds.

RESULTS AND DISCUSSIONS

External mass transfer

Since the model used here has the assumption that the external mass transfer resistance is negligibly small, we had better check the effect of agitation speed on the adsorption rate. The effective diffusivity becomes nearly constant at agitation speeds above 800 rpm. We conducted, therefore, all diffusion or counter-diffusion runs at 850 rpm. The external mass transfer coefficient, k_m, can be estimated from the initial concentration decay in the batch [8].

$$k_m = -\frac{V}{t}\ln(C_t/C_1) \tag{17}$$

As soon as the diffusion run started, the concentrations of an adsorbate were monitored periodically for about 10 minutes. k_m was calculated from the plot of $\ln(C_t/C_1)$ against t. At 850 rpm, k_m estimated from Eq. (17) was 1.8×10^{-5}m/s and the particle Sherwood number, Sh_p ($2Rk_m/D_e\varepsilon$), was 79. Since Sh_p was greater than 50, we supposed that the overall mass transfer was controlled by the intraparticle diffusion according to the criterion proposed by Neretnieks [9].

Effective Diffusivity

Figure 2 shows the fractional uptake of TPP on alumina UCl at 298K. To obtain the effective diffusivity

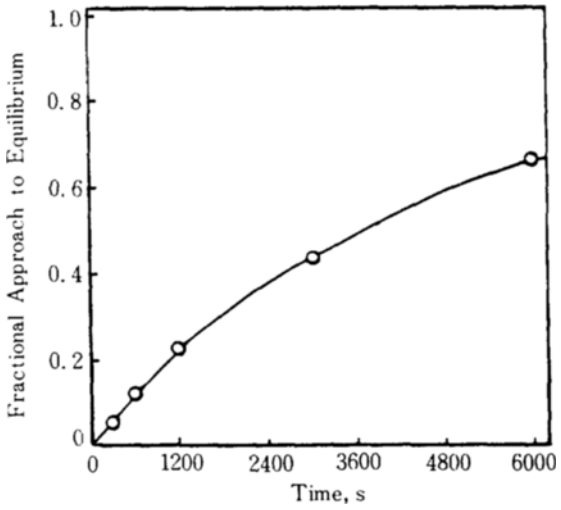

Fig. 2. Fractional uptake of TPP in cyclohexane with alumina UCl at 298K.

by applying the diffusion model to the experimental data, α should be calculated from the equilibrium concentration. Effective diffusivities measured in alumina D by varying the initial concentration of TPP are shown in Table II. The change in D_e is not significant in the concetration range of 16.4-28.8$\times 10^{-3}$ kg/m^3 of TPP. In most of sorptive diffusions, the effective diffusivity has a considerable concentration depencence since the surface coverage varys with the bulk concentration. However, when the interaction between adsorbate and adsorbent is very strong, the molecules adsorbed on the surface are immobilized so that the surface diffusion does not contribute to the effective diffusion. The weak concentration dependence of D_e reveals that the diffusion of TPP in alumina D is controlled by the pore diffusion rather than the surface diffusion [10].

Table III shows that effective diffusivities of coronene, TPP and OEP in three different aluminas. The effective diffusivity in UCl was measured to be less than those in UC2 and D. From the fact that the group parameter, $D_e/D_b\varepsilon$, increases as the ratio of molecular diameter to pore diameter decreases, it can be stated that the intraparticle diffusion may be restricted by the steric hindrance and the hydrodynamic drag. Chantong and Massoth (4). reported similar results on the effect of λ on the effective diffusivity in aluminas. For coronene,the value of D_e is in accord with that measured by them while the values of D_e of TPP and OEP are somewhat large. This discrepancy seems to come from the nonlinearity of adsorption which is assumed in this study. Table III also represents an interesting result, the group parameter, $D_e/D_b\varepsilon$ for TPP similar to that for OEP even though the critical molecule diameter of OEP is less than that of TPP [4]. This fact may be explained by the twisting of the benzene rings of TPP in order to reduce the repulsion force between the benzene rings. The real size of TPP in solution, therefore, would be smaller than its critical value.

Table 2. Effective diffusivities of TPP in alumina D at 298 K versus initial concentrations of TPP.

Initial concentration of TPP$\times 10^3$, kg/m^3	Effective diffusivity (D_e)* $\times 10^{10}$, m^2/s
16.4	1.9
20.1	2.0
28.8	1.8

* in cyclohexane

Table 3. Effective diffusivities of aromatic compounds in cyclohexane with different aluminas.

Compound	$D_b\times 10^{10}$, m^2/s	Alumina	λ ($=d_m/d_p$)	$D_e\times 10^{10}$, m^2/s	$D_e/D_b\varepsilon$
TPP	4.37	UC 1	0.38	1.0	0.40
		UC 2	0.21	1.8	0.57
		D	0.19	2.0	0.63
OEP	4.36	UC 1	0.31	1.0	0.40
		UC 2	0.17	1.8	0.57
		D	0.16	1.8	0.57
Coronene	7.45	D	0.11	2.9	0.53

D_b was estimated from the Wilke-Chang equation [15]

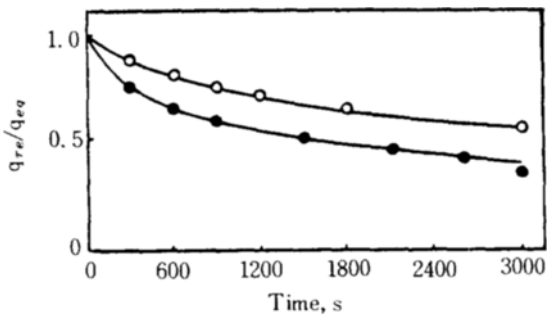

Fig. 3. Desorption curves of TPP from alumina D after injection of acetone at 298K: [7]
● : 5×10^{-7}m^3 and ○ : 1×10^{-7}m^3 of acetone.

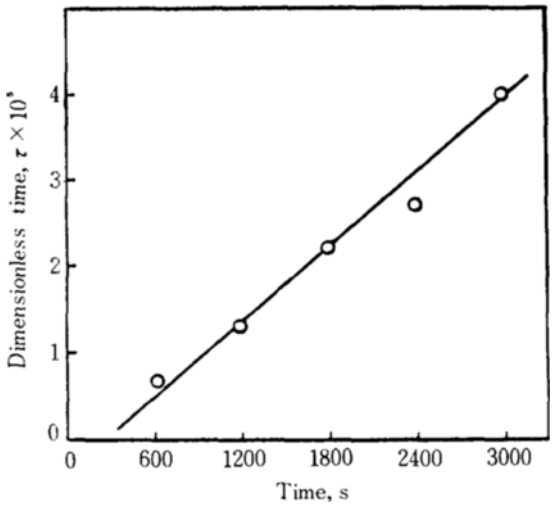

Fig. 4. Plot of τ against t for counter-diffusion data of coronene from alumina UC1 at 298K.

Counter-Diffusivity

When an aromatic compound in bulk solution is in equilibrium with that in the adsorbent, the injection of a desorbate makes the preadsorbed aromatics desorb and diffuse out from the interior to the outer surface of the particle. Figure 3 shows the remained amount of TPP after acetone was injected. In the case that 0.5×10^{-6} m^3 of acetone was injected, the amount desorbed for 5 minutes was 34% of the total uptake and 65% for 25minutes. Futhermore, the amount desorbed for 25 minutes was 47% for the injection amount of 0.1×10^{-6} m^3. This observation proves that the diffusion of acetone into pores is very fast comparing with TPP and the desorption of TPP from pore surfaces occurs instantly, as mentioned in an assumption in the theoretical section. The fact that TPP was desorbed negligibly in free solvents also supports such an assumption.

In measuring the counter-diffusivity by applying the counter-diffusion model to the experimental run data, the initial concentration in the particle, at first, should be calculated. This concentration was calculated from the desorbed amount. As shown in Fig. 4, a plot of τ against t should yield a straight line for the counter-diffusion run when the pore diffusion is dominant. The line must pass the origin theoretically, but it deviates positively from the origin. This deviation means that the arrival of desorbate molecules at pore walls takes a few minutes because the time was started from the injection of desorbate. However, the counter-diffusivity can be determined easily regardless of the deviation because this method does use only the slope of the line.

Effective diffusivities and counter-diffusivities of coronene and TPP in two different aluminas are shown in Table IV. The counter-diffusivities are about 10^{-5} times the effective diffusivities. The big differences in diffusivities can not be easily explained at present, but the possible explanation is the effect of bulk flows formed in the opposite direction in pores. This has been called as "counter-diffusion effect" and "diffusional interference" [11]. To ascertain the effect of desorbate on the counter-diffusivity, the injection amount and the type of desorbate were changed and the measured counter-diffusivities are shown in Table V. When pyridine was used as a desorbate, there are not any significant differences. Futhermore, we expected that the injection amount greatly affected the counter-diffusivity. However, counter-diffusivities did not vary

Table 4. Effective diffusivities and counter-diffusivities of TPP in cyclohexane with aluminas D and M at 298K.

	Aluminas D	M
Effective diffusivity $D_e\times10^{10}$, m^2/s	1.2	0.66
Counter-diffusivity* $D_{ec}\times10^{15}$, m^2/s	2.1	1.3

* the injection amount of acetone $=0.5\times10^{-6}$ m^3

Table 5. Counter-diffusivities of TPP and Coronene with different amount of desorbate at 298K.

Diffusant	Alumina (Solvent)	Desorbate	Injection amount $\times10^{-6}$, m^3	$D_{ec}\times10^{15}$, m^2/s
TPP	UC 1 (n-hexane)	Acetone	0.05	4.9
			0.10	5.2
			0.50	5.3
			1.00	4.5
		Pyridine	0.50	4.7
TPP	M (cyclohexane)	Acetone	0.10	1.2
			0.50	1.4
		Pyridine	0.50	1.8
Coronene	UC 1 (n-hexane)	Acetone	0.30	7.0

Table 6. Effective diffusivities and counter-diffusivities* of TPP in n-hexane with different adsorbents at 298K.

Adsorbent	Adsorbed amount of TPP $\times 10^3$, kg/kg	Remained amount after desorption $\times 10^3$, kg/kg	$D_e \times 10^{10}$, m^2/s	$D_{ec} \times 10^{15}$, m^2/s
UC 1	22	0	1.4	4.7
SA-13	35	21	1.6	6.4
SA-23	50	25	2.2	9.5

*The injection amount of acetone was 0.5×10^{-6} m^3

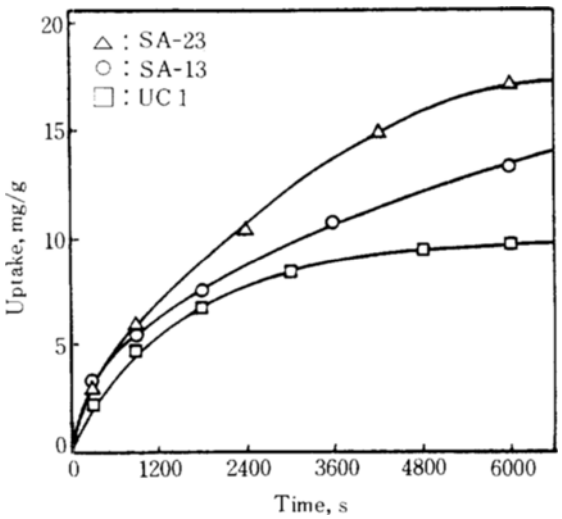

Fig. 5. Uptakes of TPP on different adsorbents at 298K.

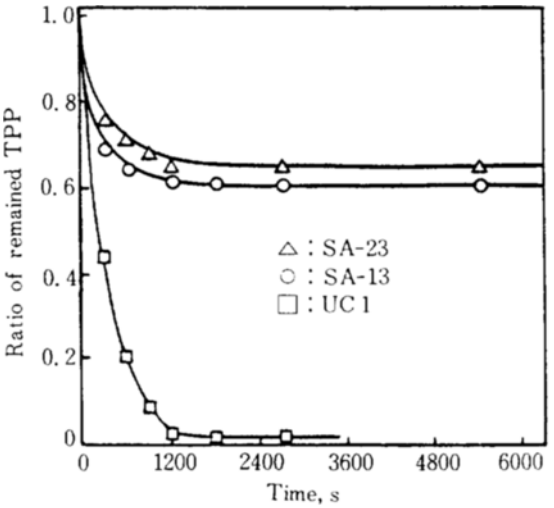

Fig. 6. Desorption curves of TPP from different adsorbents at 298K.

Table 7. Counter-diffusivities* of TPP and OEP in cyclohexane with alumina UC2 at different temperatures.

Component	Temperature, K	$D_{ec} \times 10^{15}$, m^2/s
TPP	288	1.2
	298	1.5
	313	1.5
OEP	288	1.2
	298	1.3
	313	1.5

*The injection amount of acetone was 0.5×10^{-6} m^3

with the injection amount of desorbate while the amount of aromatic compounds desorbed increases considerably. The fast desorption rate mentioned previously is somewhat surprising even though the counter-diffusivity is very low. We suppose, therefore, that the increase in the concentration gradient inside the particle is responsible for the fast diffusion rate.

Effect of Adsorption Strength and Temperature

When molecules diffuse in fine pores, the steric hindrance by pore walls has been important in the intraparticle diffusion. However, the mutual interaction between molecules and pore walls should be also considered in the sorptive diffusion encountered here. Table VI shows effective diffusivities and counter-diffusivities of TPP in different aluminas and silica-aluminas which have the the different strength of adsorption. Figure 5 and 6 show the variations of liquid phase concentration and uptake of TPP with respect to time, respectively, when the adsorber was charged with adsorbents having different adsorption strength. According to adsorption experiments performed by conventional method [1], the strength of adsorption was in the order; UC1< SA13<SA23. The TPP-adsorbed silica-aluminas were changed to blue, showing the hydrogen coordinated complex of TPP [12]. Table VI shows that D_e and D_{ec} increased in the order of the strength of adsorption. This result is contrary to the results obtained in the diffusion runs in zeolites [13, 14] and activated carbon [10]. It has been known that effective diffusivities in zeolites with very fine pores decreases with the strength of adsorption since molecules are strongly adsorbed and the immobility of adsorbed molecules becomes a cause of

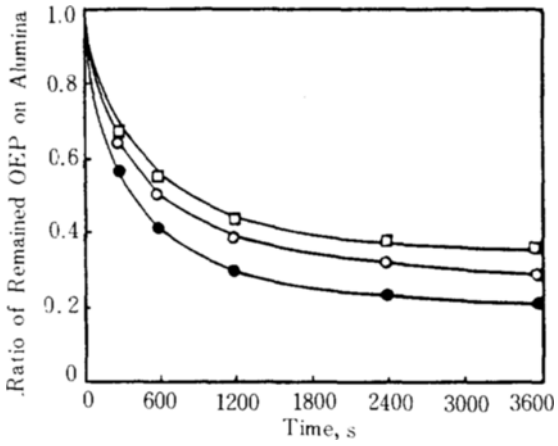

Fig. 7. Desorption curves of OEP from alumina UC2 at 288, 298 and 313K.
□ : 288K, ○ : 298K and ● : 313K

steric hindrance. Aluminas have usually larger pore sizes of about 10 nm. The immobility of molecules is not significant in aluminas since λ is less than 0.25. Even though the increase in diffusivities with the strength of adsorption can not yet be firmly explained, one of the possible explanation is the shielding effect of adsorbed molecules. The molecules adsorbed on the pore wall make it possible to prevent the diffusing molecules from interacting with the pore wall. The possibility of surface diffusion was excluded because the porphines were adsorbed strongly on alumina and localized [1].

Counter-diffusivities of TPP and OEP in alumina UC2 at 288, 298 and 313 K are shown in Table VII. D_{ec} increases slightly as the temperature increases, showing similar increasing trend in D_e [2]. Figure 7 shows the desorption curves of OEP at different temperatures. The remained amount of OEP decreases as the temperature increases. Above 313 K, experiments could not give reproducible results because of minor impurities in solvents.

CONCLUSIONS

Effective diffusivities and counter-diffusivities of porphines were determined by applying two diffusion models to the experimental data. The measured counter-diffusivity was about 10^{-5} times the effective diffusivity. The possible explanation for such a decrease was the existance of counter-flows formed in the opposite direction. The effective diffusivity was not affected by the bulk concentration. This weak concentration dependence reveals that the pore diffusion is predominant in the intraparticle diffusion of aromatic compounds in aluminas. Measured counter-diffusivities increased in the order of UC1<SA-13<SA-23, this is, in the order of the strength of adsorption. We suppose that the shielding effect of molecules adsorbed on the surface is the possible cause for the increase in diffusivity.
The counter-diffusivities increased slightly as the temperature increased. This was similar increasing tendency in the effective diffusivity.

ACKNOWLEDGEMENT

The author gratefully acknowledge the financial support of Korea Science and Engineering Foundation.

NOMENCLATURE

C_1 : bulk concentration at t=0, kg/m^3
C_0 : concentration in particles at t=0, kg/m^3 and hypothetical concentration after desorption
C_r : concentration within particle at radius r, kg/m^3
C_t : bulk concentration at time t, kg/m^3
C_∞ : equilibrium concentration after adsorption or desorption, kg/m^3
D_a : apparent diffusivity, m^2/s
D_e : effective diffusivity, m^2/s
D_{ec} : counter-diffusivity, m^2/s
d_p : average pore diameter, nm
d_m : critical molecular diameter, nm
K : equilibrium adsorption constant
k_m : external mass transfer coefficient, m/s
N_p : number of particles
OEP : octa-ethylporphine
q : adsorption amount, kg/kg
q_n : roots of a transcendental equation, Eq. (7)
q_{eq} : equilibrium adsorption amount, kg/kg
q_{re} : remained amount of adsorbate after desorption, kg/kg
q_∞ : adsorption amount at t=∞, kg/kg
R : average particle radius, m
r : radial distance, m
Sh_p : Sherwood number
t : time, s
TPP : tetra-phenylporphine
V : volume of bulk solution, m^3

Greeks

α : constant
ρ : particle density, kg/m^3
ε : porosity
λ : diameter ratio
τ : dimensionless time

REFERENCES

1. Chantong, A.: Ph. D. Thesis, University of Utah, 1982.

2. Seo, G. and Massoth, F.E.: *AIChE J.*, **31,** 494 (1985).
3. Satterfield, C.N., Katzer, J.R. and Vieth, W.R.: *Ind. Eng. Chem. Fundam.*, **10,** 478 (1971).
4. Chantong, A. and Massoth, F.E.: *AIChE J.* **29,** 725 (1983).
5. van Vuuren, D.S., Stander, C.M. and Glasser, D.: *AIChE J.*, **30,** 593 (1984).
6. Crank, J.: "The Mathematics of Diffusion", Clarenden Press, Oxford, 1975.
7. Seo, G.: *J. Korean Inst. Chem. Eng.*, **22,** 1 (1984).
8. Furusawa, T. and Smith, J.M.: *Ind. Eng. Chem. Fundam.*, **12,** 197 (1973).
9. Neretnieks, I.: *Chem. Eng. Sci.*, **31,** 107 (1976).
10. Moon, H. and Lee, W.K.: *J. Colloid Interface Sci.*, **96,** 162 (1983).
11. Moon, H. and Lee, W.K.: Paper presented at the 1984's spring meeting of the Korean Institute of Chemical Engineers, Seoul, Korea, 1984.
12. Cady, S.C. and Pinavaia, T.J.: *Inorg. Chem.*, **17,** 1501(1978).
13. Praser, B.D. and Ma, Y.H.: *AIChE J.*, **23,** 303 (1977).
14. Satterfield, C.N., Colton, C.K. and Pitcher, W.H.: *AIChE* J., **19.,** 623 (1973).
15. Reid, R.C., Prausnitz, J.M. and Sherwood, T.K.: "The Properties of Gases and Liquids", 3rd ed., MaGraw-Hill, New York, 1977.